Lysozyme resistance in *C. difficile* is dependent on two peptidoglycan deacetylases

Gabriela M. Kaus[1], Lindsey F. Snyder[2], Ute Müh[1], Matthew J. Flores[3], David L. Popham[3], & Craig D. Ellermeier [1,2,4]

[1] Department of Microbiology and Immunology
Carver College of Medicine
University of Iowa
431 Newton Rd
Iowa City, IA 52242

[2] Interdisciplinary Graduate Program in Genetics
University of Iowa
Iowa City, IA 52242, USA

[3] Department of Biological Sciences
Virginia Tech
Blacksburg, VA 24061, USA

[4]Corresponding author
craig-ellermeier@uiowa.edu
319-384-4565

Running title: PdaV & PgdA confer lysozyme resistance in *C. difficile*

Keywords: σ factors, cell envelope, stress response, signal transduction, gene expression

Abstract:

Clostridioides (Clostridium) difficile is a major cause of hospital-acquired infections leading to antibiotic-associated diarrhea. *C. difficile* exhibits a very high level of resistance to lysozyme. Bacteria commonly resist lysozyme through modification of the cell wall. In *C. difficile* σ^V is required for lysozyme resistance and σ^V is activated in response to lysozyme. Once activated σ^V, encoded by *csfV*, directs transcription of genes necessary for lysozyme resistance. Here we analyze the contribution of individual genes in the *csfV* regulon to lysozyme resistance. Using CRISPR-Cas9 mediated mutagenesis we constructed in-frame deletions of single genes in the *csfV* operon. We find *pdaV,* which encodes a peptidoglycan deacetylase, is partially responsible for lysozyme resistance. We then performed CRISPR inhibition (CRISPRi) to identify a second peptidoglycan deacetylase, *pgdA*, that is important for lysozyme resistance. Deletion of either *pgdA* or *pdaV* resulted in modest decreases in lysozyme resistance. However, deletion of both *pgdA* and *pdaV* resulted in a 1000-fold decrease in lysozyme resistance. Further, muropeptide analysis revealed loss of either PgdA or PdaV had modest effects on peptidoglycan deacetylation but loss of both PgdA and PdaV resulted in almost complete loss of peptidoglycan deacetylation. This suggests that PgdA and PdaV are redundant peptidoglycan deacetylases. We also use CRISPRi to compare other lysozyme resistance mechanisms and conclude that peptidoglycan deacetylation is the major mechanism of lysozyme resistance in *C. difficile*.

Importance:

Clostridioides difficile is the leading cause of hospital-acquired diarrhea. *C. difficile* is highly resistant to lysozyme. We previously showed that the *csfV* operon is required for lysozyme resistance. Here we use CRISPR-Cas9 mediated mutagenesis and CRISPRi knockdown to show that peptidoglycan deacetylation is necessary for lysozyme resistance and is the major lysozyme resistance mechanism in *C. difficile.* We show that two peptidoglycan deacetylases in *C. difficile* are partially redundant and are required for lysozyme resistance. PgdA provides an intrinsic level

55 of deacetylation and PdaV, encoded as part of the *csfV* operon, provides lysozyme-induced
56 peptidoglycan deacetylation.
57

Introduction:

Clostridioides difficile is a Gram-positive, anaerobic, opportunistic pathogen. *C. difficile* infections are the most common cause of hospital-acquired diarrhea worldwide, with disease severity ranging from mild diarrhea to severe cases of pseudomembranous colitis (1, 2). *C. difficile* infections commonly affect patients whose normal gut microbiota has been perturbed by antibiotic treatment. Disease is primarily mediated through two exotoxins, TcdA and TcdB (3, 4). Both toxins are glucosyltransferases that glucosylate Rho family GTPases, leading to cytoskeletal defects in the cell and collapse of tight junctions, which in turn leads to inflammation and cell death of colonic epithelial cells, ultimately resulting in gastrointestinal distress (5, 6).

The bacterial cell wall provides the structure and protection needed for survival in the host environment. In *C. difficile,* the cell envelope is composed of a thick layer of peptidoglycan, a crystalline S-layer, and multiple polysaccharides attached to the cell wall (PS-II and PS-III) (7–10). Presumably to cause an infection *C. difficile* must survive the host immune factors present in the colon and elevated during the inflammatory response. One abundant host defense factor is lysozyme, a component of the innate immune system that cleaves the β-1,4-glycosidic linkage between the GlcNAc and MurNAc residues in the peptidoglycan backbone leading to lysis and cell death (11, 12). *C. difficile* peptidoglycan has unusual features including a high level of GlcNAc *N*-deacetylation and an abundance of 3-3 peptide cross-links (13). Deacetylation of peptidoglycan is a common lysozyme resistance mechanism in a wide variety of bacteria (14).

C. difficile senses and responds to lysozyme via the ECF σ factor σ^V (15, 16). σ^V homologs are also found in multiple other Firmicutes including *Bacillus subtilis* and *Enterococcus faecalis* (17–19). The activity of σ^V is inhibited by RsiV, a membrane bound anti-σ factor. In *B. subtilis* and *E. faecalis,* RsiV is degraded in the presence of lysozyme (20, 21). In *C. difficile,* σ^V is encoded by *csfV*, which is found in a 7-gene operon (Fig. S1). The σ^V operon also encodes *pdaV*, a peptidoglycan deacetylase and *lbpA* (*cdr20291_1409*), an *rsiV* ortholog containing a putative lysozyme-binding domain (15).

In order to survive and cause infection, many bacteria modify their cell wall components to resist lysozyme and other cell wall stressors. One mechanism used by multiple organisms including *C. difficile* is alteration of the net charge of the cell envelope through D-alanyl esterification (22–24). A second common resistance mechanism is direct inhibition of lysozyme via lysozyme inhibitor proteins (25–28). The *C. difficile* σ^V regulon includes two putative lysozyme inhibitor proteins (RsiV and LbpA) and the *dltABCD* operon which is responsible for D-alanyl esterification (15, 24). Lastly, many bacteria modify their peptidoglycan backbone to prevent lysozyme from accessing the β-1,4-glycosidic linkage (29, 30).

The peptidoglycan backbone can be modified in four ways including acetylation and deacetylation of both the GlcNAc or MurNAc residues (29). *B. subtilis, E. faecalis, Staphylococcus aureus* and *Neisseria gonorrhoeae* resist killing by lysozyme through addition of an acetyl group at the C-6 position of the MurNAc residue, by an O-acetyltransferase frequently encoded by *oatA* (14, 29, 31). *Lactobacillus plantarum* has been shown to have an O-acetyltransferase that modifies the GlcNAc residue (32). Alternatively, other organisms including *B. cereus, B. anthracis, E. faecalis* and *Streptococcus pneumoniae* utilize polysaccharide deacetylases to remove the N-acetyl group on the GlcNAc residue at the C-2 position (14, 29). In *B. subtilis* PdaC has been shown to remove the acetyl group on the MurNAc residue (33). The σ^V regulon in *C. difficile* and *E. faecalis* contains a polysaccharide deacetylase (*pdaV* and *pgdA,* respectively) that deacetylates the GlcNAc resides (15, 34). In *B. subtilis* the σ^V operon includes *oatA* leading to O-acetylation (19).

Previously, we reported that σ^V is required for lysozyme resistance in *C. difficile* and this was partially mediated by deacetylation of peptidoglycan (15). Here we report that the high level of lysozyme resistance and peptidoglycan deacetylation in *C. difficile* is mediated in large part by two peptidoglycan deacetylases, PdaV and PgdA. PgdA provides intrinsic basal deacetylation while PdaV is induced in response to lysozyme, increasing the overall level of deacetylation.

Results:

σ^V is required for expression of the *csfV* operon

σ^V, encoded by *csfV (sigV),* in *C. difficile* is necessary for lysozyme resistance (15). Previous studies of *csfV* were performed in a *C. difficile* CD630 derivative, JIR8094, and used a Targetron insertion in *csfV* which is polar on downstream genes (15). Because Targetron mutagenesis does not allow dissecting the role of individual genes, we sought to use CRISPR-Cas9 mutagenesis to construct in frame deletions of genes within the *csfV* operon to determine their contributions to lysozyme resistance. Since σ^V is required for its own expression, disruption of *csfV* blocked expression of the entire operon (15, 35, 36). To confirm that σ^V is required for expression of the *csfV* operon in *C. difficile* strain R20291, we used CRISPR-Cas9 mediated mutagenesis to construct an in-frame deletion of *csfV* (37). To monitor σ^V activity, we used a P_{pdaV}::*rfp* reporter plasmid to measure activation of the *csfV* operon in response to lysozyme (35). Cultures were grown to mid-log phase, then incubated with lysozyme to induce expression of P_{pdaV}. In the wildtype strain, we observed a lysozyme-dependent increase in fluorescence indicating increased expression of the P_{pdaV}::*rfp* reporter (Fig. 1). Consistent with previous studies, lysozyme did not induce P_{pdaV}::*rfp* expression in the Δ*csfV* mutant (Fig. 1). In fact, basal levels of P_{pdaV}::*rfp* expression were significantly (~80-fold) lower in the Δ*csfV* mutant, indicating that σ^V is required for expression of the *csfV* operon and there is a high basal level expression of the *csfV* operon (15, 35).

Activation of σ^V increases lysozyme resistance

We developed a liquid culture, 96-well format MIC assay for measuring *C. difficile* sensitivity to lysozyme. Unfortunately, high concentrations of lysozyme (>1 mg/mL) cause turbidity in the medium, preventing a direct read of culture growth. Instead, we evaluated growth by spotting an aliquot on to an agar plate and incubating overnight. Wildtype *C. difficile* is highly

resistant to lysozyme with an MIC of 8 mg/ml. We found that the Δ*csfV* mutant was 4-fold more sensitive to lysozyme than the wildtype (Fig. 2A).

This MIC assay tests the ability of *C. difficile* to survive exposure to a specific concentration of lysozyme. However, during an infection *C. difficile* likely encounters a gradient of lysozyme concentrations. To reproduce a similar environment, we pre-incubated cultures with a range of sub-inhibitory concentrations of lysozyme prior to exposing them to high levels of lysozyme in the MIC assay. We observed that when incubated with sub-inhibitory lysozyme concentrations, the MIC of wildtype *C. difficile* increases in response to both the concentration and length of exposure (Fig. 2). We found that exposure of wildtype *C. difficile* to 20 µg/ml of lysozyme, for 3 and 5 hours increased lysozyme resistance 2- and 4-fold respectively (Fig. 2A). When the concentration of lysozyme in the pre-incubation step was altered, we saw a dose-dependent increase in the resistance level of the wildtype strain (Fig. 2B). However, we did not observe a change in the MIC of the Δ*csfV* mutant with either increased incubation time or increased lysozyme concentrations, indicating that σ^V is required for inducible lysozyme resistance (Fig. 2). We found that pre-incubation for 5 hours with 20 µg/ml lysozyme led to maximum lysozyme resistance in a wildtype with an MIC of 32 mg/ml, which was 16-fold higher than the Δ*csfV* mutant MIC of 2 mg/ml (Fig. 2). A similar observation was made with the Δ*csfV* operon mutant (Fig. S2A).

PdaV and PgdA are redundant

σ^V is required for transcription of genes necessary for lysozyme resistance (15). We sought to dissect the contribution of individual genes to lysozyme resistance. Lysozyme resistance levels were determined using the MIC assay described above. When the samples were grown without pretreatment, we found that when either *csfV* alone or the full *csfV* operon is deleted, the mutant *C. difficile* is 8-fold more sensitive to lysozyme than the wildtype strain (Fig. 3A).

When *pdaV,* a peptidoglycan deacetylase, is deleted we see a 2-fold reduction in lysozyme sensitivity (Fig. 3A). Additionally, we found that when the Δ*pdaV* mutant was complemented with *pdaV* on a plasmid, lysozyme resistance was restored to levels at or above the wildtype MIC (Fig. 3B). Previous work found that peptidoglycan from a *csfV* mutant in JIR8094 remains highly deacetylated (~75%) (15). Thus, we sought to identify what other factors may be contributing to the high degree of deacetylation. *C. difficile* encodes 7 putative polysaccharide deacetylases that contain predicted transmembrane domains (13, 38). We used CRISPR inhibition (CRISPRi) to knockdown expression of each deacetylase individually and screened for changes in lysozyme sensitivity (39). For each deacetylase gene we constructed two plasmids with different sgRNAs and as a negative control we included a negative control sgRNA that had no target in the *C. difficile* genome. We tested the CRISPRi plasmids in a *ΔcsfV* operon strain because we sought to observe differences that are independent of the *csfV* response and it lacked *pdaV* (Fig. S2B). Six of the genes when targeted by CRISPRi had no effect on lysozyme resistance (Fig. S2B). However, we identified one putative deacetylase gene, *cdr20291_1371,* (hereafter referred to as *pgdA* [peptidoglycan deacetylase]) that when knocked down in the Δ*csfV* operon background resulted in a ~100-fold decrease in the level of lysozyme resistance relative to the parent strain (Fig. S2B).

To confirm the results of the CRISPRi knockdown screen, we constructed an in-frame deletion of *pgdA.* When only *pgdA* was deleted we observed a modest 2-fold decrease in lysozyme resistance, similar to the 2-fold decrease observed when *pdaV* is deleted (Fig. 3A). However, when both *pgdA* and *pdaV* are deleted we observed a ~1000-fold decrease in lysozyme resistance (Fig. 3A). This data suggests that *pgdA* and *pdaV* are redundant and that either one is sufficient to confer high level of lysozyme resistance in *C. difficile*. To further support the redundant phenotype of *pgdA* and *pdaV,* we exogenously expressed *pdaV* in the Δ*pgdA* Δ*pdaV* double mutant. We found that exogenous expression of *pdaV* in a Δ*pgdA* Δ*pdaV* double mutant

185 restored lysozyme resistance to 2 mg/ml, similar to a *ΔpgdA* mutant (Fig. 3B). We were unable to
186 complement with *pgdA* as we had difficulty cloning in *E. coli* and continuously obtained frameshift
187 mutations within *pgdA*.

188 Additionally, we used CRISPRi to knockdown expression of *pgdA* in another *C. difficile*
189 strain, JIR8094 an erythromycin sensitive derivative of *C. difficile* CD630 (40). When *pgdA* was
190 knocked down in a wildtype background we observed a ~2-fold reduction in lysozyme resistance
191 (Fig. S3). When *pgdA* was knocked down in a JIR8094 *csfV*-null strain we observed a ~100-fold
192 decrease in lysozyme resistance (Fig. S3). This indicates that loss of both PdaV and PgdA results
193 in a large decrease in lysozyme resistance in multiple *C. difficile* strains.

194 To determine if expression of *pgdA* was lysozyme-inducible, we constructed a P_{pgdA}-*rfp*
195 fusion. We then tested the effect of increasing lysozyme concentrations on P_{pgdA}-*rfp* expression.
196 We did not observe an increase in P_{pgdA}-*rfp* expression in response to increasing lysozyme
197 concentrations suggesting *pgdA* expression is not controlled by lysozyme (Fig. S4). This is
198 consistent with previous microarray experiments that did not show altered expression of *pgdA* by
199 lysozyme (15).

200

201 **PdaV and PgdA are the major peptidoglycan deacetylases in *C. difficile***

202 Next, we sought to identify the acetylation state of peptidoglycan from strains lacking one
203 or both of the deacetylases contributing to lysozyme resistance. We purified peptidoglycan from
204 wildtype, Δ*pgdA,* Δ*pdaV,* and Δ*pgdA* Δ*pdaV* strains. Peptidoglycan was digested with
205 mutanolysin, and muropeptides were separated by charge using reversed-phase HPLC (Fig. 4A).
206 Muropeptide structures were either previously determined or were newly determined using mass
207 spectrometry (15). The peptidoglycan purified from wildtype strain R20291 was made up of
208 muropeptides containing mostly glucosamine (i.e. deacetylated) rather than N-acetyl-
209 glucosamine residues (Fig. 4B and Table 1). Analysis of the peptidoglycan from the Δ*pdaV* mutant

210 revealed the level of deacetylation remained relatively unchanged compared to the wildtype strain
211 (Fig. 4B and Table 1). When *pgdA* was deleted, we observed decreases in the muropeptides
212 containing glucosamine residues corresponding with an increase in muropeptides containing
213 GlcNAc residues (Fig. 4B and Table 1). In the Δ*pgdA* Δ*pdaV* mutant we saw a drastic increase in
214 the amount of GlcNAc residues and a concomitant decrease in glucosamine residues, with the
215 overall percentage of muropeptides containing GlcNAc increasing ~15-fold relative to the wildtype
216 strain. For example, we saw in the double mutant the deacetylated tri-gly muropeptides (peak 4)
217 are almost completely absent, concomitant with an increase in acetylated tri-gly muropeptides
218 (peak 3) (Table 1). This suggests that both PdaV and PgdA are major peptidoglycan deacetylases
219 in *C. difficile*.
220
221 **RsiV and LbpA act as inhibitors of lysozyme**
222 In *B. subtilis,* RsiV binding to lysozyme leads to σ^V activation (21). In addition to RsiV, the
223 σ^V operon in *C. difficile* encodes for CDR1409 (CD1560 in JIR8094), an RsiV ortholog hereafter
224 referred to as *lbpA* for lysozyme-binding protein A. LbpA is 58% identical to *C. difficile* RsiV and
225 contains a putative lysozyme binding domain but lacks the σ-binding domain (Fig. S5). We sought
226 to determine if RsiV and LbpA contribute to lysozyme resistance via direct inhibition of lysozyme.
227 To determine if RsiV and LbpA can inhibit lysozyme we performed an *in vitro* lysozyme inhibition
228 assay. We purified 6xHis-RsiV and 6xHis-LbpA from *E. coli*. Peptidoglycan from *M. lysodeikticus*
229 was incubated with lysozyme and varying concentrations of RsiV or LbpA. We observed that when
230 the ratio of RsiV to lysozyme was greater than 1:1, the activity of lysozyme was inhibited, and the
231 peptidoglycan remained intact (Fig. 5A and Fig. S6). When equimolar ratios of lysozyme and RsiV
232 were used most of the lysozyme activity was blocked (Fig. 5A and Fig. S6). Similarly, LbpA
233 inhibited lysozyme activity when used in excess or equimolar ratio to lysozyme (Fig. 5A and Fig.
234 S6). This suggests that both RsiV and LbpA can bind and inhibit lysozyme activity *in vitro*.

To investigate the effect of LbpA on lysozyme resistance we constructed an in-frame deletion of *lbpA* and tested the effect on the lysozyme MIC. We did not observe any effect on lysozyme resistance (Fig. S7A). We did not attempt to construct a deletion of *rsiV* since it would lead to constitutive activation of σ^V and thus would be difficult to dissect the contribution of lysozyme inhibition versus the effect on σ^V activity. Instead, to further investigate the role of these putative lysozyme inhibitors we tested the ability of both proteins to alter the resistance level *in vivo* by exogenous expression from the P_{xyl} promoter. We found that exogenous expression of *rsiV* or *lbpA* does not alter lysozyme resistance in a Δ*csfV* operon background (Fig. S7B). We hypothesized that inhibition of lysozyme may contribute to lysozyme resistance only when lysozyme concentrations are low. Thus, to detect differences, we used our most lysozyme sensitive strain, Δ*pgdA* Δ*pdaV.* We observed that exogenous expression of *rsiV* or *lbpA* increases lysozyme resistance 4- and 2-fold respectively, relative to the Δ*pgdA* Δ*pdaV* parent strain (Fig. 5B). Together these data indicate that both RsiV and LbpA can inhibit lysozyme *in vitro* and confer resistance to low levels of lysozyme *in vivo*.

Contribution of other cell wall modification to lysozyme resistance

Several other factors have been implicated in lysozyme resistance in *C. difficile* including the S-layer and d-alanylation of teichoic acids (10, 36). We sought to compare the contribution of these other lysozyme resistance mechanisms to the role of peptidoglycan deacetylation. To do this we used CRISPRi to knockdown expression of the *dltABCD* operon, which alters the charge of teichoic acids, and expression of *slpA,* which encodes the major S-layer proteins. We found that when the *dltABCD* operon is knocked down, the MIC decreases ~16-fold from 8 to 0.5 mg/mL (Fig. S8). Similarly, upon knocking down *slpA* we lower the MIC to ~2 mg/ml, a ~4-fold change from wildtype (Fig. S8). As a control for CRISPR-silencing versus gene deletion, we also knocked down the *csfV* operon and observed ~4-8-fold decrease in lysozyme resistance. Thus, knocking

down each of these genes results in decreased lysozyme resistance similar to that of the *ΔcsfV* mutant. In conclusion, our data suggests that multiple factors contribute to lysozyme resistance. Nevertheless, deacetylation is the single most important mechanism, where deletion of the two key deacetylases achieves an MIC shift of ~1000-fold.

Discussion

Lysozyme is an important component of the innate immune system and one of the first lines of defense against bacteria. In order to avoid killing by lysozyme, many bacteria modify cell wall properties including peptidoglycan and cell surface charge. We find *C. difficile* encodes both an endogenous lysozyme resistance and an inducible lysozyme resistance mechanism. The inducible lysozyme resistance is primarily mediated by the ECF σ factor σ^V. In response to lysozyme, σ^V upregulates expression of lysozyme resistance mechanisms including the Dlt pathway, a peptidoglycan deacetylase (PdaV), and putative lysozyme inhibitor proteins (RsiV and LbpA) (15, 36). Additionally, a high basal level of peptidoglycan deacetylation and the crystalline S-layer contribute to lysozyme resistance (10). Here we show that together these modifications help confer a high level of lysozyme resistance.

One common mechanism of lysozyme resistance used by bacteria is modification of the acetylation state of peptidoglycan to prevent cleavage at the β-(1-4) linkage by lysozyme. Peptidoglycan modifications include addition or removal of acetyl groups from either the MurNAc or GlucNAc residues on the peptidoglycan backbone (29, 41). In many pathogens, including *S. aureus* and *L. monocytogenes* O-acetylation is important for resistance to lysozyme and virulence (42, 43). Multiple organisms, including *C. difficile*, *B. subtilis* and *E. faecalis* modify peptidoglycan in a σ^V dependent manner in response to lysozyme (15, 18, 19, 31, 44). In *B. subtilis,* the σ^V operon includes an O-acetylase, *oatA* which is responsible for acetylating the MurNAc residues in peptidoglycan (19, 31). Additionally, the *dlt* operon in *B. subtilis*, responsible for D-alanylation of teichoic acids, is regulated by σ^V (31, 45). Mutations in either *oatA* or the *dlt* operon results in

~2-fold decrease in lysozyme resistance (19, 31). Similarly, the σ^V regulon in *E. faecalis* includes *pgdA*, a peptidoglycan deacetylase that contributes to lysozyme resistance (44, 46). *E. faecalis* also depends on OatA and the Dlt pathway for lysozyme resistance, however these are σ^V-independent (18, 34, 44).

Previous work demonstrated that *C. difficile* peptidoglycan is highly deacetylated (13). We had shown that deacetylation can be increased in response to lysozyme via increased activity of σ^V which was presumably mediated by PdaV (15). Here, we have identified an additional peptidoglycan deacetylase, PgdA, that plays a critical role in lysozyme resistance. When both *pgdA* and *pdaV* are deleted, only a small percentage of the peptidoglycan is deacetylated and the level of lysozyme resistance is drastically decreased. This suggests that the high level of deacetylation observed in *C. difficile* is required for lysozyme resistance. Our data indicated either PgdA or PdaV are sufficient for high levels of lysozyme resistance, with loss of either *pgdA* or *pdaV* resulting in modest 2-fold decreases in lysozyme resistance. When *pgdA* alone was deleted, we detected a decrease in total percentage of deacetylated glucosamine residues. Interestingly, we did not observe a change in total percentage of deacetylated residues in the absence of *pdaV*. This is likely because the samples were grown in the absence of lysozyme and therefore the σ^V response was not activated. However, it is also clear from this analysis that even in the absence of lysozyme there is a significant contribution of PdaV to deacetylation likely due to high basal level expression of *pdaV*. In fact, we observed high basal level expression of the *pdaV* reporter in a wildtype strain and deletion of *csfV* resulted in a marked decrease in P_{pdaV}-*rfp* reporter signal. Taken together our data suggest that either PdaV or PgdA are sufficient for peptidoglycan deacetylation and lysozyme resistance in *C. difficile*.

We have shown that exposing cultures to sub-inhibitory levels of lysozyme prior to incubation with high levels of lysozyme allows the cells to increase the lysozyme MIC in a σ^V-dependent manner. This indicates that the modifications made by the σ^V regulon during exposure to sub-inhibitory lysozyme permit the bacteria to increase their ability to survive when exposed to

high levels of lysozyme. Lysozyme activates the σ^V-mediated modifications including increased deacetylation and D-alanylation of teichoic acids (36).

One of the unique features of the *C. difficile csfV* operon is the presence of two proteins, RsiV and LbpA, which can bind lysozyme. RsiV functions as an anti-σ factor and can inhibit σ^V activity (19). In contrast, LbpA lacks the σ^V-binding domain. We find that both RsiV and LbpA inhibit lysozyme activity *in vitro*. Our data also show that exogenous production of either RsiV or LbpA in a lysozyme sensitized strain (*ΔpgdA ΔpdaV*) increases lysozyme resistance. The ability of RsiV and LbpA to inhibit lysozyme activity and increase the MIC in a sensitive strain indicate a possible role for lysozyme inhibitors in *C. difficile*. It is unclear how rapidly the peptidoglycan and lipoteichoic acids can be modified to increase lysozyme resistance. As a *C. difficile* infection is established, the toxins elicit an inflammatory response recruiting neutrophils to the site of infection increasing the concentration of lysozyme. We hypothesize that the lysozyme inhibitors may be important early in infection to sequester lysozyme allowing the cell additional time for surface modifications such as increased deacetylation.

Materials and Methods:

Bacterial strains, media and growth conditions. Bacterial strains are listed in Table 2. *C. difficile* strains used in this study are derivatives of R20291. *C. difficile* was grown in or on tryptone-yeast (TY) medium supplemented as needed with thiamphenicol at 10 μg/ml (Thi_{10}), kanamycin at 50 μg/ml, or cefoxitin at 50 μg/ml. TY consisted of 3% tryptone, 2% yeast extract and 2% agar (for solid medium). *C. difficile* strains were maintained at 37°C in an anaerobic chamber (Coy Laboratory products) in an atmosphere of 10% H_2, 5% CO_2, and 85% N_2.

E. coli strains were grown in LB medium at 37°C with chloramphenicol at 10 μg/ml and ampicillin at 100 μg/ml as needed. LB contained 1% tryptone, 0.5% yeast extract, 0.5% NaCl and 1.5% agar (for solid medium).

337

338 **Plasmid and bacterial strain construction**. All plasmids are listed in Table 3 and Table S1.
339 Plasmids were constructed using Gibson Assembly (New England Biolabs, Ipswich, MA). Regions
340 of plasmids constructed using PCR were verified by DNA sequencing. Oligonucleotide primers
341 used in this work were synthesized by Integrated DNA Technologies (Coralville, IA) and are listed
342 in Table S2. All plasmids were propagated using OmniMax-2 T1R as a cloning host. CRISPR-
343 Cas9 deletion plasmids were passaged through *E. coli* strain MG1655, before transformation into
344 *B. subtilis* strain BS49. The CRISPR-Cas9 deletion plasmids which harbor the $oriT_{(Tn916)}$ origin of
345 transfer, were then introduced into *C. difficile* strains by conjugation (37). All other plasmids (RP4
346 *oriT traJ* origin of transfer) were transformed into *E. coli* strain HB101/pRK24, then introduced into
347 *C. difficile* by conjugation (47).

348 CRISPR-Cas9 plasmids were built on the backbone of pJK02 (37). Initial constructs
349 expressed *cas9* under P_{tet} control. The final construct, pCE641, placed *cas9* under P_{xyl} control.
350 The P_{tet} regulatory element was removed from pJK02 by digestion with PacI and XhoI and
351 replaced with a *xylR*-P_{xyl} fragment amplified by PCR of R20291 chromosomal DNA. Donor regions
352 for homology were made by separately amplifying regions ~500 bp upstream and ~500 bp
353 downstream of the gene of interest. The resulting regions were cloned into the NotI and XhoI
354 restriction sites in pCE641 by Gibson Assembly. The algorithm provided by Benchling was used
355 to design sgRNAs targeting each deleted gene (48). Guide parameters were set to default
356 conditions to identify a 20-nucleotide guide with the PAM set to NGG. sgRNA fragments were
357 amplified by PCR from pCE641, using an upstream primer that introduces the altered guide and
358 inserted at the KpnI and MluI sites of the pCE641-derivative with the appropriate homology region.

359 For CRISPRi constructs, the algorithm provided by Benchling was used to design sgRNAs
360 as described above. Final candidates were selected to be high scoring and bind to the non-coding
361 strand in the first third of the gene sequence. The sequences for sgRNAs are summarized in

Table S3. sgRNA fragments were amplified by PCR from pIA33, using an upstream primer that introduces the altered guide and inserted at the MscI and NotI sites of the pIA33 (39).

Peptidoglycan purification. Peptidoglycan was purified from 100 ml cultures grown to an OD_{600} of 0.6 to 0.8 in TY broth. Peptidoglycan was purified as previously described (Ho 2014). Briefly, cells were pelleted by centrifugation and supernatant was discarded. The cells were boiled in 4% sodium dodecyl sulfate (SDS) for 1 hr. Samples were pelleted and supernatant was discarded. Samples were washed in sterile water 6 times to remove SDS. Samples were digested with DNaseI (NEB) and RNase (Sigma-Aldrich) for 2 hrs at 37°C to remove nucleotides and then digested with Trypsin (Sigma-Aldrich) for 16 hrs at 37°C. Teichoic acids were removed by resuspending the samples in 1 ml 49% hydrofluoric acid (VWR) rocking for 48 hrs 4°C. Samples were subsequently washed extensively in sterile water. The peptidoglycan was digested for 16 hrs with 125 units Mutanolysin (Sigma-Aldrich) as previously described (49). Muropeptides were separated and purified using HPLC and analyzed by MALDI-TOF MS as previously described (15).

Protein expression and purification. Cultures of *E. coli* BL21λDE3 Rosetta containing an expression plasmid for either RsiV or LbpA were diluted 1:100 in 100 ml LB supplemented with 10 μg/ml chloramphenicol and 100 μg/ml ampicillin. Samples were grown at 30°C to an OD_{600} of 0.6 then induced with 1mM IPTG and grown for an additional 4 hrs at 30°C. Cells were chilled on ice and pelleted by centrifugation at 2500 x *g*. Cell pellets were stored at -80°C until time for purification. Cells were thawed on ice in 2 ml lysis buffer (50 mM Tris HCl 250 mM NaCl, 10 mM imidazole, 3 mM Triton X-100 pH 8.0). Cells were lysed by sonication and lysate was centrifuged at 17,000 x *g* to pellet cell debris. Clarified lysate was added to 500 μl nickel resin slurry (Thermo) and incubated rocking at 4°C for 30 minutes to bind 6xHis-tagged protein. The resin was washed

five times with 2 ml wash buffer (50 mM Tris-HCl, 250 mM NaCl, 20 mM imidazole, 0.3 mM Triton X-100 pH 8.0). To elute protein, resin was incubated with 500 μl elution buffer (50 mM Tris-HCl, 250 mM NaCl, 250 mM imidazole, 0.03 mM Triton X-100 pH 8.0) rocking at 4°C for 15 minutes. Samples were centrifuged, and supernatant collected.

Lysozyme activity assay. Lysozyme activity was measured by following the degradation of a commercially available PG preparation (lyophilized *Micrococcus lysodeikticus* cells from Sigma). Increasing concentrations of purified RsiV or LbpA were mixed with lysozyme (final concentration in assay, 10 μg/ml) in 50 μl in a 96 well plate. The reaction was started by the addition of 50 μl PG substrate (*M. lysodeikticus* PG suspension in 50 mM Na phosphate, pH 7, 100 mM NaCl at an optical density of 1.8). PG lysis was monitored at 450 nm, every minute for 30 min (M200 Pro plate reader, Tecan).

Lysozyme MIC determination. Overnight cultures were subcultured and grown to late log phase (OD_{600} of 1.0), then diluted in TY to 10^6 CFU/ml. For samples that were pre-incubated with lysozyme, lysozyme was added at the time and concentration indicated. A series of lysozyme concentrations was prepared in a 96-well plate in 50 μl TY broth. Wells were inoculated with 50 μl of the dilute late log culture (i.e. 0.5 x 10^5 CFU/well) and grown at 37°C for 16 hrs. Each well was then sampled by removing 10 μl and diluting 1:10 in TY broth; 5 μl of this dilution was spotted onto TY agar and incubated at 37°C for 24 hrs. The MIC was defined as the lowest concentration of lysozyme at which 5 or fewer colonies were found per spot.

Fixation protocol. Cells were fixed as previously described (35, 50). Briefly, a 500 μl aliquot of cells in growth medium was added to 100 μl 16% paraformaldehyde (Alfa Aesar) and 20 μl of 1M $NaPO_4$ buffer (pH 7.4). The sample was mixed, removed from the chamber, and incubated in the

412 dark at room temperature for 60 minutes. The samples were washed 3 times with phosphate-
413 buffered saline (PBS), resuspended in 100 μl PBS, and left in the dark for a minimum of 3 hrs to
414 allow for maturation of the chromophore.
415
416 **Fluorescence measurements with a plate reader.** Fluorescence from bulk samples was
417 measured using an Infinite M200 Pro plate reader (Tecan, Research Triangle Park, NC) as
418 previously described (35, 39). Briefly, fixed cells in PBS were added to a 96-well microtiter plate
419 (black, flat optical bottom). Fluorescence was recorded as follows: excitation at 554 nm, emission
420 at 610 nm, and gain setting 140. The cell density (OD600) was also recorded and used to
421 normalize the fluorescence reading.
422
423 **Acknowledgements**
424 This work was supported by the National Institutes of Allergy and Infectious Disease NIH
425 R01AI087834 to CDE and a graduate fellowship T32AI007511 to GMK. We thank Joe Sorg for
426 providing the CRISPR mutagenesis plasmid. We would also like to thank members of the
427 Ellermeier and Weiss labs for helpful comments.
428
429
430
431

Figure Legends:

Figure 1. Wildtype (GMK208) or Δ*csfV* (GMK211) strains containing a P_{pdaV}-*rfp* reporter plasmid were grown to an OD_{600} of 0.3, incubated with lysozyme for 1 hr, then fixed and removed from the anaerobic chamber. Samples were exposed to air overnight to allow for maturation of the chromophore. Fluorescence was measured via a plate reader.

Figure 2. Pre-incubation with a sub-inhibitory concentration of lysozyme increases resistance level. A) Overnight cultures of wildtype or Δ*csfV* (CDE2966) were sub-cultured and grown for ~8hrs; 20 μg/ml lysozyme was added for the duration indicated prior to set up of the lysozyme MIC plates. B) Overnight cultures were sub-cultured and grown to an OD_{600}= 0.3; varying sub-inhibitory concentrations of lysozyme were added as indicated and cultures incubated for ~5 hrs prior to set up of MIC.

Figure 3. A) Overnight cultures were sub-cultured into TY medium and grown to an OD_{600}= 0.3; 20 μg/ml lysozyme was added and incubated for 5 hrs prior to set up of MIC (WT, R20291; *ΔpgdA,* GMK241; *ΔpdaV,* GMK152; *ΔcsfV* operon, GMK157; *ΔcsfV* operon *ΔpgdA,* GMK243; *ΔpdaV ΔpgdA,* GMK301). B) Strains carrying either P_{xyl}-*pdaV* (pCE618) or an empty vector (pAP114) were constructed (*ΔcsfV* operon *ΔpgdA* pAP114, GMK312; *ΔcsfV* operon *ΔpgdA* pCE618, GMK313; *ΔpdaV ΔpgdA* pAP114, GMK314; *ΔpdaV ΔpgdA* pCE618, GMK315; *ΔpdaV* pAP114, GMK316; *ΔpdaV* pCE618, GMK317; *ΔcsfV* operon pAP114, GMK174; *ΔcsfV* operon pCE618, GMK177). Overnight cultures were sub-cultured into TY Thi_{10} medium supplemented with 1% xylose. Cultures were grown to an OD_{600}= 1.0 and a lysozyme MIC was set up with 1% xylose.

Figure 4. Peptidoglycan was purified from cultures grown to mid-log (OD_{600}= 0.6-0.8). Peptidoglycan was digested with mutanolysin. Fragments were separated using reversed-phase

457 HPLC and structures determined using mass spectrometry. B) Total percentages of deacetylated
458 residues are shown for strains indicated (WT, R20291; *ΔpdaV,* GMK152; *ΔpgdA,* GMK241; *ΔpgdA*
459 *ΔpdaV,* GMK301).
460
461
462 **Figure 5.** A) Peptidoglycan from *M. lysodeikticus* was combined with 10 µg/ml lysozyme and
463 purified RsiV or LbpA. The A_{450} was monitored every minute for 30 minutes to determine
464 degradation of lysozyme. Degradation after 30 minutes is shown. B) Overnight cultures were sub-
465 cultured into TY Thi_{10} medium supplemented with 1% xylose and grown to OD_{600}= 1.0 and a
466 lysozyme MIC was set up with 1% xylose. A one-way ANOVA showed effect of the inhibitor
467 proteins on lysozyme resistance was significant, F (2,9)= 9.8, *p*= 0.0055.
468
469 **Figure S1.** Organization of the *csfV* operon in *C. difficile* strain R20291.
470
471 **Figure S2.** Contribution of putative polysaccharide deacetylases to the lysozyme MIC. A) MICs
472 of in-frame deletions of individual genes (WT, R20291; *ΔcsfV,* CDE2966; *ΔcsfV* operon,
473 GMK157). Overnight cultures were sub-cultured and grown to an OD_{600} of 0.3, incubated with 20
474 µg/ml lysozyme for 5 hrs, then MICs were determined. B) Putative polysaccharide deacetylases
475 were screened using CRISPRi knockdown in a *ΔcsfV* operon strain (*cdr1160,* LS136, LS137;
476 *cdr1293*, LS142, LS143; *pgdA,* LS131, LS132; *cdr2485,* LS144, LS145; *cdr2613,* LS140, LS141;
477 *cdr3106,* LS138, LS139; *cdr3115,* LS129, LS130; CRISPRi negative control, LS134). Overnight
478 cultures grown with 1% xylose were sub-cultured in TY supplemented with 1% xylose and grown
479 to an OD_{600} of 1.0, then MICs were determined.
480
481 **Figure S3.** CRISPRi knockdown of *pgdA* was tested in JIR8094 strain backgrounds (JIR8094
482 CRISPRi negative control, GMK358; JIR8094 CRISPRi *pgdA*, GMK256; JIR8094 *csfV::ltrB::ermB*

CRISPRi negative control, GMK361; JIR8094 *csfV::ltrB::ermB* CRISPRi *pgdA*, GMK359). Overnight cultures grown with 1% xylose were sub-cultured in TY supplemented with 1% xylose and grown to an OD_{600} of 1.0, then MICs were determined.

Figure S4. *pgdA* is not activated by lysozyme. Strains carrying either P_{pdaV}-*rfp* (GMK208) or P_{pgdA}-*rfp* (LS155) were sub-cultured and grown to an OD_{600} of 0.3 then incubated with varying concentrations of lysozyme for 1 hr. Cultures were fixed, removed from the chamber and exposed to air overnight to allow for maturation of the chromophore. Fluorescence was measured via a plate reader.

Figure S5. Alignment of RsiV from *B. subtilis*, RsiV from *C. difficile,* and LbpA. The σ-factor binding domain is noted. Underlined residues indicate the transmembrane domain.

Figure S6. RsiV and LbpA were overexpressed and purified from *E. coli.* Peptidoglycan from *M. lysodeikticus* was combined with 10 μg/ml hen egg white lysozyme and various concentrations of purified RsiV or LbpA. The A_{450} was monitored every minute for 30 minutes to determine degradation of lysozyme.

Figure S7. Contribution of individual genes in the *csfV* operon on lysozyme resistance. A) MICs of in-frame deletions of individual genes (WT, R20291; *ΔlbpA,* UM303). Overnight cultures were sub-cultured and grown to an OD_{600} of 0.3, incubated with 20 μg/ml lysozyme for 5 hrs, then MICs were determined. B) Single genes were exogenously expressed from a xylose-inducible expression vector in a Δ*csfV* operon mutant strain (*ΔcsfV* operon EV, GMK174; *ΔcsfV* operon P_{xyl}-*rsiV*, GMK176; *ΔcsfV* operon P_{xyl}-*lbpA,* GMK178). Cultures were grown with 1% xylose to an OD_{600} of 1.0 then MICs were determined.

Figure S8. CRISPRi knockdown was used to determine the contribution of *slpA* and the *dltABCD* operon to lysozyme resistance in a wildtype background, 2 different sgRNAs were tested for *dltABCD* and *csfV* (EV, LS134; *slpA,* GMK344; *dltABCD,* GMK345, GMK346; *csfV,* GMK347, GMK348). Overnight cultures grown with 1% xylose were sub-cultured in TY supplemented with 1% xylose and grown to an OD_{600} of 1.0 then MICs were determined.

Table 1. Muropeptide Analysis

Peak #[a]	Muropeptide Structure[b]	m/z[c] Predicted	m/z[c] Actual	Area (%) of each muropeptide peak (mean ± SD) WT (n = 3)	Δ*pdaV* *(n = 4)*	Δ*pgdA* (n = 4)	Δ*pgdA*Δ*pdaV* *(n = 4)*
A	Tri	893.5	892.9	0 ± 0.0	0 ± 0.1	1 ± 0.1	2 ± 0.2
1	Tri, deAc	851.4	851.4	1 ± 0.1	1 ± 0.1	1 ± 0.1	0 ± 0.1
3	Tri-Gly	950.5	949.9	2 ± 0.1	2 ± 0.2	4 ± 0.7	14 ± 1.0
4	Tri-Gly, deAc	908.4	908.4	6 ± 0.7	6 ± 0.8	6 ± 0.6	0 ± 0.1
6	Tetra	964.4	963.9	7 ± 0.7	7 ±0.9	12 ±1.4	14 ± 1.7
7	Tetra, deAc	922.4	922.4	25 ± 3.0	24 ± 2.2	17 ± 1.4	1 ± 0.4
C	Tri-Tri-Gly	1802.7	1802.5	0 ± 0.4	0 ± 0.2	1 ± 0.2	12 ± 0.4
D	Tri-Tri	1745.7	1745.5	1 ± 0.6	2 ± 0.7	2 ± 0.4	3 ± 0.2
11a	Tri-Tri-Gly, deAcX2	1718.7	1718.8	5 ± 0.4	5 ± 0.4	4 ± 0.7	0 ± 0.2
11b	Tri-Tri, deAcX2	1661.7	1661.8	1 ± 0.1	1 ±0.1	1 ± 0.2	1 ± 0.5
E	Tri-, Tetra-Gly	1873.8	1873.5	1± 1.8	1 ±1.7	5 ± 0.4	22 ± 2.5
12	Tri-Tetra	1816.8	1816.5	4 ± 0.7	4 ± 0.5	9 ± 1.3	2 ± 2.5
14	Tri-Tetra, deAcX1	1774.8	1774.8	5 ± 0.6	5 ± 0.4	5 ± 0.3	1 ± 0.1
15a	Tri-Tetra, deAcX2	1732.7	1732.7	20 ± 1.0	20 ± 1.1	13 ± 0.9	0 ± 0.2
16	Tri-Tetra, deAcX1	1774.8	1774.8	1 ± 0.2	1 ± 0.2	1 ± 0.1	0 ± 0.0
F	Tri-Tetra	1816.8	1816.4	0 ± 0.5	0 ± 0.4	1 ± 0.1	7 ± 0.2
17	Tri-Tetra, deAcX2	1732.7	1732.7	7 ± 0.7	6 ± 0.9	3 ± 1.0	0 ± 0.1
G	Tetra-Tetra	1887.8	1887.4	1 ± 1.1	0 ± 0.9	2 ± 1.8	7 ± 0.6
17a	Tetra-Tetra	1887.8	1887.7	1 ± 0.3	1 ± 0.6	2 ± 0.2	0 ± 0.1
19	Tetra-Tetra, deAcX2	1803.8	1803.6	2 ± 0.4	2 ± 0.2	2 ± 0.2	1 ± 0.4
20	Tetra-Tetra, deAcX1	1845.8	1845.7	5 ± 0.0	5 ± 0.5	3 ± 0.2	1 ± 0.5
H	Tri-Tri-Tri-Gly	2654.9	2655.6	0 ± 0.0	0 ± 0.0	0 ± 0.3	5 ± 0.3
21	Tetra-Tetra, deAcX2	1803.8	1803.6	3 ± 0.2	3± 0.2	2 ± 0.1	1 ± 1.0
I	Tri-Tri-Tetra	2669.0	2669.7	0 ± 0.2	0 ± 0.3	0 ± 0.3	4 ± 0.4
23	Tri-Tri-Tetra, deAcX3	2543.1	2542.8	3 ± 0.3	3 ± 0.3	1 ± 0.2	1 ± 1.0

[a] Peak name as identified in (13) or as labeled in Fig. 4.

[b] Peptide side chains are indicated; each peptide is attached to a disaccharide. deAcX1, deAcX2, and deAcX3 refer to one, two, or three deacetylated disaccharides, respectively.

[c] m/z for $[M+Na]^+$ ion.

523 **Table 2. Strains**

Strain	Genotype and Description	Reference*
E. coli		
OmniMAX – 2 T1^{R}	F´ [*pro*AB+ *lac*Iq *lac*ZΔM15 Tn10(Tet^{R}) Δ(*ccd*AB)] *mcr*A Δ(*mrr-hsd*RMS-*mcr*BC) Φ80*lac*ZΔM15 Δ(*lac*ZYA-*arg*F) U169 *end*A1 *rec*A1 *sup*E44 *thi*-1 *gyr*A96 *rel*A1 *ton*A *pan*D.	Invitrogen
XL1-Blue	*endA1 gyrA96*(nal^{R}) *thi-1 recA1 relA1 lac glnV44* [F' *proAB*$^{+}$ *lacI*^{q} Δ(*lacZ*)M15] *hsdR17*(r_K^- m_K^+) Tn*10*(Tet^{R})]	
HB101/pRK24	F− *mcrB mrr hsdS20*(r_B^- m_B^-) *recA13 leuB6 ara-14 proA2 lacY1 galK2 xyl-5 mtl-1 rpsL20*	(51)
BL21λDE3 Rosetta	*huA2 [lon] ompT gal (λ DE3) [dcm]* Δ*hsdS λ DE3 = λ sBamHIo* Δ*EcoRI-B int::(lacI::PlacUV5::T7) i21* Δ*nin5* / pRARE (CamR)	Novagen
MG1655	Wild-type *E. coli*	
GMK231	BL21λDE3 Rosetta pCE596 (P_{T7}-*6xhis-rtev-rsiV*$^{70-289}$ *amp)*	
GMK232	BL21λDE3 Rosetta pCE469 (P_{T7}-*6xhis-lbpA* $^{35-251}$ *amp)*	
B. subtilis		
BS49	Tn*916* donor strain	
C. difficile		
JIR8094	Spontaneous erythromycin-sensitive derivative of strain 630 (Ribotype 012)	(40)
TCD20	JIR8094 *csfV::ltrB::ermB*	(15)
GMK358	JIR8094 pIA34 (negative control)	
GMK356	JIR8094 pCE655 (CRISPRi *pgdA-1*)	
GMK361	JIR8094 *csfV::ltrB::ermB* pIA34 (negative control)	
GMK359	JIR8094 *csfV::ltrB::ermB* pCE655 (CRISPRi *pgdA-1*)	
R20291	Wild-type *C. difficile* strain from UK outbreak (ribotype 027)	(52)
CDE2966	R20291 *ΔcsfV*	
GMK157	R20291 *ΔcsfV* operon (*pdaV-cdr1411)*	
GMK152	R20291 Δ*pdaV*	
UM303	R20291 Δ*lbpA*	
GMK241	R20291 *ΔpgdA*	
GMK243	R20291 *ΔcsfV* operon *ΔpgdA*	
GMK301	R20291 *ΔpgdA ΔpdaV*	
GMK208	R20291 pRAN738 (P_{pdaV}-*rfp)*	
GMK211	R20291 *ΔcsfV* pRAN738 (P_{pdaV}-*rfp)*	
GMK174	R20291 *ΔcsfV* operon pAP114	
GMK176	R20291 *ΔcsfV* operon pCE617 (P_{xyl}-*rsiV)*	
GMK177	R20291 *ΔcsfV* operon pCE618 (P_{xyl}-*pdaV)*	
GMK178	R20291 *ΔcsfV* operon pCE619 (P_{xyl}-*lbpA)*	
GMK314	R20291 *ΔpdaV ΔpgdA* pAP114 (P_{xyl}-*rfp)*	
GMK315	R20291 *ΔpdaV ΔpgdA* pCE618 (P_{xyl}-*pdaV*)	
GMK316	R20291 *ΔpdaV* pAP114 (P_{xyl}-*rfp*)	
GMK317	R20291 *ΔpdaV* pCE618 (P_{xyl}-*pdaV*)	
GMK248	R20291 *ΔcsfV* operon *ΔpgdA* pAP114 (P_{xyl}-*rfp*)	
GMK249	R20291 *ΔcsfV* operon *ΔpgdA* pCE617 (P_{xyl}-*rsiV*)	
GMK250	R20291 *ΔcsfV* operon *ΔpgdA* pCE619 (P_{xyl}-*lbpA*)	

LS155	R20291 pCE670 (P_{pgdA}-*rfp*)	
LS129	R20291 Δ*csfV* operon pCE653 (CRISPRi *cdr3115-1*)	
LS130	R20291 Δ*csfV* operon pCE654 (CRISPRi *cdr3115-2*)	
LS131	R20291 Δ*csfV* operon pCE655 (CRISPRi *pgdA-1*)	
LS132	R20291 Δ*csfV* operon pCE656 (CRISPRi *pgdA-2*)	
LS134	R20291 Δ*csfV* operon pIA34 (CRISPRi negative control)	
LS136	R20291 Δ*csfV* operon pCE657 (CRISPRi *cdr1160-1*)	
LS137	R20291 Δ*csfV* operon pCE658 (CRISPRi *cdr1160-2*)	
LS138	R20291 Δ*csfV* operon pCE659 (CRISPRi *cdr3106-1*)	
LS139	R20291 Δ*csfV* operon pCE660 (CRISPRi *cdr3106-2*)	
LS140	R20291 Δ*csfV* operon pCE661 (CRISPRi *cdr2613-1*)	
LS141	R20291 Δ*csfV* operon pCE662 (CRISPRi *cdr2613-2*)	
LS142	R20291 Δ*csfV* operon pCE663 (CRISPRi *cdr1293-1*)	
LS143	R20291 Δ*csfV* operon pCE664 (CRISPRi *cdr1293-1*)	
LS144	R20291 Δ*csfV* operon pCE651(CRISPRi *cdr2485-1*)	
LS145	R20291 Δ*csfV* operon pCE652 (CRISPRi *cdr2485-2*)	
GMK344	R20291 pIA39 (CRISPRi *slpA-1*)	(39)
GMK345	R20291 pCE738 (CRISPRi *dlt-1*)	
GMK346	R20291 pCE739 (CRISPRi *dlt-1*)	
GKM347	R20291 pCE746 (CRISPRi *csfV-1*)	
GMK348	R20291 pCE747 (CRISPRi *csfV-2*)	

524 *This study unless otherwise noted.

525 **Table 3. Plasmids**

Plasmid	Relevant Features	Reference*
pRPF185	*E. coli-C. difficile* shuttle vector with tetracycline-inducible promoter. P_{tet}::*gusA cat CD6ori RP4oriT-traJ pMB1ori*	(53)
pRAN738	P_{pdaV}::*mCherryOpt cat*	(35)
pAP114	P_{xyl}::*mCherryOpt cat*	(39)
pCE617	P_{xyl}::*rsiV cat*	
pCE618	P_{xyl}::*pdaV cat*	
pCE619	P_{xyl}::*lbpA cat*	
pCE596	P_{T7}-*6xhis-rtev-rsiV*$^{80-289}$ *amp*	
pCE469	P_{T7}-*6xhis-rtev-lbpA*$^{35-251}$ *amp*	
pCE641	P_{xyl}::*Cas9-opt ΔrasP* P_{gdh}::*sgRNA-rasP catP*	
pCE651	P_{xyl}::*dCas9-opt Pgdh::sgRNA-cdr2495-1 catP*	
pCE652	P_{xyl}::*dCas9-opt Pgdh::sgRNA-cdr2495-2 catP*	
pCE653	P_{xyl}::*dCas9-opt Pgdh::sgRNA-cdr3115-1 catP*	
pCE654	P_{xyl}::*dCas9-opt Pgdh::sgRNA-cdr3115-2 catP*	
pCE655	P_{xyl}::*dCas9-opt Pgdh::sgRNA-pgdA-1 catP*	
pCE656	P_{xyl}::*dCas9-opt Pgdh::sgRNA-pgdA-2 catP*	
pCE657	P_{xyl}::*dCas9-opt Pgdh::sgRNA-cdr1160-1 catP*	
pCE658	P_{xyl}::*dCas9-opt Pgdh::sgRNA-cdr1160-2 catP*	
pCE659	P_{xyl}::*dCas9-opt Pgdh::sgRNA-cdr3106-1 catP*	
pCE660	P_{xyl}::*dCas9-opt Pgdh::sgRNA-cdr3106-2 catP*	
pCE661	P_{xyl}::*dCas9-opt Pgdh::sgRNA-cdr2613-1 catP*	
pCE662	P_{xyl}::*dCas9-opt Pgdh::sgRNA-cdr2613-2 catP*	
pCE663	P_{xyl}::*dCas9-opt Pgdh::sgRNA-cdr1293-1 catP*	
pCE664	P_{xyl}::*dCas9-opt Pgdh::sgRNA-cdr1293-2 catP*	
pCE670	P_{pgdA}::*mCherry Opt cat*	
pIA34	P_{xyl}::*dCas9-opt* P_{gdh}::*sgRNA-neg catP*	
pIA39	P_{xyl}::*dCas9-opt* P_{gdh}::*sgRNA-slpA-2 catP*	
pCE738	P_{xyl}::*dCas9-opt* P_{gdh}::*sgRNA-dlt-1 catP*	
pCE739	P_{xyl}::*dCas9-opt* P_{gdh}::*sgRNA-dlt-2 catP*	
pCE746	P_{xyl}::*dCas9-opt* P_{gdh}::*sgRNA-csfV-1 catP*	
pCE747	P_{xyl}::*dCas9-opt* P_{gdh}::*sgRNA-csfV-2 catP*	
pYZ101	P_{tet}::*Cas9-opt ΔcsfV Pgdh::sgRNA-csfV catP*	
pGK112	P_{tet}::*Cas9-opt ΔpdaV Pgdh::sgRNA-pdaV catP*	
pGK115	P_{tet}::*Cas9-opt ΔpdaV-cdr1411* P_{gdh}::*sgRNA-csfV catP*	

pCE678	P_{xyl}*::Cas9-opt ΔpgdA* P_{gdh}*::sgRNA-pgdA-2 catP*	
pIA16	P_{tet}*::Cas9-opt ΔlbpA 9* P_{gdh}*::sgRNA-lbpA catP*	

*This study unless otherwise noted.

References

1. Rupnik M, Wilcox MH, Gerding DN. 2009. *Clostridium difficile* infection: new developments in epidemiology and pathogenesis. Nat Rev Micro 7:526–536.
2. Pépin J, Valiquette L, Cossette B. 2005. Mortality attributable to nosocomial *Clostridium difficile*-associated disease during an epidemic caused by a hypervirulent strain in Quebec. CMAJ 173:1037–1042.
3. Lyras D, Connor JRO, Howarth PM, Sambol SP, Glen P, Phumoonna T, Poon R, Adams V, Vedantam G, Gerding DN, Rood JI. 2009. Toxin B is essential for virulence of *Clostridium difficile*. Nature 458:1176–1179.
4. Voth DE, Ballard JD. 2005. *Clostridium difficile* Toxins: Mechanism of Action and Role in Disease. Clin Microbiol Rev 18:247–263.
5. Shen A. 2012. *Clostridium difficile* Toxins : Mediators of Inflammation. J Innate Immun 149–158.
6. Kelly CP, LaMont JT. 1998. *Clostridium difficile* Infection. Annu Rev Med 49:375–90.
7. Percy MG, Gründling A. 2014. Lipoteichoic Acid Synthesis and Function in Gram-Positive Bacteria. Annu Rev Microbiol 68:81–100.
8. Reid CW, Vinogradov E, Li J, Jarrell HC, Logan SM, Brisson JR. 2012. Structural characterization of surface glycans from *Clostridium difficile*. Carbohydr Res 354:65–73.
9. Ganeshapillai J, Vinogradov E, Rousseau J, Weese JS, Monteiro MA. 2008. *Clostridium difficile* cell-surface polysaccharides composed of pentaglycosyl and hexaglycosyl phosphate repeating units. Carbohydr Res 343:703–710.
10. Kirk JA, Banerji O, Fagan RP. 2017. Characteristics of the *Clostridium difficile* cell envelope and its importance in therapeutics. Microb Biotechnol 10:76–90.
11. Callewaert L, Michiels C. 2010. Lysozymes in the animal kingdom. J Biosci.
12. Chipman DM, Sharon N. 1969. Mechanism of Lysozyme Action. Science (80-) 165:454–465.

555 13. Peltier J, Courtin P, El Meouche I, Lemée L, Chapot-Chartier MP, Pons JL. 2011.
556 *Clostridium difficile* has an original peptidoglycan structure with a high level of N-
557 acetylglucosamine deacetylation and mainly 3-3 cross-links. J Biol Chem 286:29053–
558 29062.
559 14. Davis KM, Weiser JN. 2011. Modifications to the Peptidoglycan Backbone Help Bacteria
560 To Establish Infection. Infect Immun 79:562–570.
561 15. Ho TD, Williams KB, Chen Y, Helm RF, Popham DL, Ellermeier CD. 2014. *Clostridium*
562 *difficile* extracytoplasmic function σ factor σ^V regulates lysozyme resistance and is
563 necessary for pathogenesis in the hamster model of infection. Infect Immun 82:2345–55.
564 16. Ho TD, Ellermeier CD. 2011. PrsW Is Required for Colonization, Resistance to
565 Antimicrobial Peptides , and Expression of Extracytoplasmic Function σ Factors in
566 *Clostridium difficile*. Infect Immun 79:3229–3238.
567 17. Staron A, Sofia HJ, Dietrich S, Ulrich LE, Liesegang H, Mascher T. 2009. The third pillar
568 of bacterial signal transduction : classification of the extracytoplasmic function (ECF) σ
569 factor protein family. Mol Microbiol 74:557–581.
570 18. Benachour A, Muller C, Dabrowski-coton M, Breton Y Le, Giard J, Rince A, Auffray Y,
571 Hartke A. 2005. The *Enterococcus faecalis* SigV Protein Is an Extracytoplasmic Function
572 Sigma Factor Contributing to Survival following Heat, Acid, and Ethanol Treatments. J
573 Bacteriol 187:1022–1035.
574 19. Ho TD, Hastie JL, Intile PJ, Ellermeier CD. 2011. The *Bacillus subtilis* Extracytoplasmic
575 Function σ Factor σ^V Is Induced by Lysozyme and Provides Resistance to Lysozyme. J
576 Bacteriol 193:6215–6222.
577 20. Hastie JL, Williams KB, Ellermeier CD. 2013. The activity of σ^V, an Extra-Cytoplasmic
578 Function σ factor of *Bacillus subtilis*, is controlled by a regulated proteolysis of the anti-σ
579 factor RsiV. J Bacteriol 195:3135–3144.
580 21. Hastie JL, Williams KB, Sepúlveda C, Houtman JC, Forest KT, Ellermeier CD. 2014.

Evidence of a Bacterial Receptor for Lysozyme: Binding of Lysozyme to the Anti-σ Factor RsiV Controls Activation of the ECF σ Factor σ^V. PLoS Genet 10.

22. Neuhaus FC, Baddiley J. 2003. A Continuum of Anionic Charge: Structures and Functions of D- Alanyl- Teichoic Acids in Gram- Positive Bacteria. Microbiol Mol Biol Rev 67:686.

23. Nizet V. 2006. Antimicrobial Peptide Resistance Mechanisms of Human Bacterial Pathogens. Curr Issues Mol Biol 11–26.

24. McBride SM, Sonenshein AL. 2011. The *dlt* operon confers resistance to cationic antimicrobial peptides in *Clostridium difficile*. Microbiology 157:1457–1465.

25. Callewaert L, Herreweghe JM Van, Vanderkelen L, Leysen S, Voet A, Michiels CW. 2012. Guards of the great wall : bacterial lysozyme inhibitors. Trends Microbiol 20:501–510.

26. Leysen S, Van Herreweghe JM, Callewaert L, Heirbaut M, Buntinx P, Michiels CW, Strelkov S V. 2011. Molecular basis of bacterial defense against host lysozymes: X-ray structures of periplasmic lysozyme inhibitors PliI and PliC. J Mol Biol 405:1233–1245.

27. Monchois V, Abergel C, Sturgis J, Jeudy S, Claverie JM. 2001. *Escherichia coli ykfE* ORFan Gene Encodes a Potent Inhibitor of C-type Lysozyme. J Biol Chem 276:18437–18441.

28. Yum S, Kim MJ, Xu Y, Jin XL, Yoo HY, Park JW, Gong JH, Choe KM, Lee BL, Ha NC. 2009. Structural basis for the recognition of lysozyme by MliC, a periplasmic lysozyme inhibitor in Gram-negative bacteria. Biochem Biophys Res Commun 378:244–248.

29. Vollmer W. 2008. Structural variation in the glycan strands of bacterial peptidoglycan. FEMS Microbiol Rev 32:287–306.

30. Vollmer W, Tomasz A. 2000. The *pgdA* gene encodes for a peptidoglycan N-acetylglucosamine deacetylase in *Streptococcus pneumoniae*. J Biol Chem 275:20496–20501.

607 31. Guariglia-oropeza V, Helmann JD. 2011. *Bacillus subtilis* σ^V Confers Lysozyme
608 Resistance by Activation of Two Cell Wall Modification Pathways, Peptidoglycan O-
609 Acetylation and D -Alanylation of Teichoic Acids. J Bacteriol 193:6223–6232.
610 32. Rolain T, Bernard E, Beaussart A, Degand H, Courtin P, Egge-Jacobsen W, Bron PA,
611 Morsomme P, Kleerebezem M, Chapot-Chartier MP, Dufrêne YF, Hols P. 2013. O-
612 glycosylation as a novel control mechanism of peptidoglycan hydrolase activity. J Biol
613 Chem 288:22233–22247.
614 33. Kobayashi K, Putu Sudiarta I, Kodama T, Fukushima T, Ara K, Ozaki K, Sekiguchi J.
615 2012. Identification and characterization of a novel polysaccharide deacetylase C (PdaC)
616 from *Bacillus subtilis*. J Biol Chem 287:9765–9776.
617 34. Hébert L, Courtin P, Torelli R, Sanguinetti M, Chapot-Chartier MP, Auffray Y, Benachour
618 A. 2007. *Enterococcus faecalis* constitutes an unusual bacterial model in lysozyme
619 resistance. Infect Immun 75:5390–5398.
620 35. Ransom EM, Ellermeier CD, Weiss DS. 2015. Use of mCherry red fluorescent protein for
621 studies of protein localization and gene expression in *Clostridium difficile*. Appl Environ
622 Microbiol 81:1652–1660.
623 36. Woods EC, Nawrocki KL, Suárez JM, McBride SM. 2016. The *Clostridium difficile* Dlt
624 Pathway Is Controlled by the Extracytoplasmic Function Sigma Factor σ^V in Response to
625 Lysozyme. Infect Immun 84:1902–1916.
626 37. McAllister KN, Bouillaut L, Kahn JN, Self WT, Sorg JA. 2017. Using CRISPR-Cas9-
627 mediated genome editing to generate *C. difficile* mutants defective in selenoproteins
628 synthesis. Sci Rep 1–12.
629 38. Paley S, Karp PD. 2017. Update notifications for the BioCyc collection of databases.
630 Database (Oxford) 2017:1–4.
631 39. Müh U, Pannullo AG, Weiss DS, Ellermeier CD. 2019. A Xylose-Inducible Expression
632 System and a CRISPR Interference Plasmid for Targeted Knockdown of Gene

633 Expression in *Clostridioides difficile*. J Bacteriol 201:1–12.

634 40. O'Connor JR, Lyras D, Farrow KA, Adams V, Powell DR, Hinds J, Cheung JK, Rood JI.
635 2006. Construction and analysis of chromosomal *Clostridium difficile* mutants. Mol
636 Microbiol 61:1335–51.

637 41. Ragland SA, Criss AK. 2017. From bacterial killing to immune modulation: Recent
638 insights into the functions of lysozyme. PLoS Pathog 13:1–22.

639 42. Bera A, Herbert S, Jakob A, Vollmer W, Götz F. 2005. Why are pathogenic staphylococci
640 so lysozyme resistant? The peptidoglycan O-acetyltransferase OatA is the major
641 determinant for lysozyme resistance of *Staphylococcus aureus*. Mol Microbiol 55:778–
642 787.

643 43. Aubry C, Goulard C, Nahori MA, Cayet N, Decalf J, Sachse M, Boneca IG, Cossart P,
644 Dussurget O. 2011. OatA, a peptidoglycan O-acetyltransferase involved in *Listeria*
645 *monocytogenes* immune escape, is critical for virulence. J Infect Dis 204:731–740.

646 44. Jeune L, Torelli R, Sanguinetti M, Giard J, Hartke A, Auffray Y, Benachour A. 2010. The
647 Extracytoplasmic Function Sigma Factor SigV Plays a Key Role in the Original Model of
648 Lysozyme Resistance and Virulence of *Enterococcus faecalis*. PLoS One 5.

649 45. Asai K, Yamaguchi H, Kang CM, Yoshida KI, Fujita Y, Sadaie Y. 2003. DNA microarray
650 analysis of *Bacillus subtilis* sigma factors of extracytoplasmic function family. FEMS
651 Microbiol Lett 220:155–160.

652 46. Benachour A, Ladjouzi R, Le Jeune A, Hébert L, Thorpe S, Courtin P, Chapot-Chartier
653 MP, Prajsnar TK, Foster SJ, Mesnage S. 2012. The Lysozyme-Induced Peptidoglycan N-
654 Acetylglucosamine Deacetylase *pgda* (EF1843) Is Required for *Enterococcus faecalis*
655 Virulence. J Bacteriol 194:6066–6073.

656 47. Kirk JA, Fagan RP. 2016. Heat shock increases conjugation efficiency in Clostridium
657 difficile. Anaerobe.

658 48. Benchling. 2018. Benchling. San Francisco, CA.

659 49. Popham DL, Helin J, Costello CE, Setlow P. 1996. Analysis of the peptidoglycan
660 structure of *Bacillus subtilis* endospores. J Bacteriol 178:6451–6458.
661 50. Ransom EM, Williams KB, Weiss DS, Ellermeier CD. 2014. Identification and
662 Characterization of a Gene Cluster Required for Proper Rod Shape, Cell Division, and
663 Pathogenesis in *Clostridium difficile.* J Bacteriol 196:2290–2300.
664 51. Trieu-Cuot P, Arthur M, Courvalin P. 1987. Origin, Evolution and Dissemination of
665 Antibiotic Resistance Genes. Microbiol Sci 4:263–6.
666 52. Stabler RA, He M, Dawson L, Martin M, Valiente E, Corton C, Lawley TD, Sebaihia M,
667 Quail MA, Rose G, Gerding DN, Gibert M, Popoff MR, Parkhill J, Dougan G, Wren BW.
668 2009. Comparative genome and phenotypic analysis of *Clostridium difficile* 027 strains
669 provides insight into the evolution of a hypervirulent. Genome Biology 10:1–15.
670 53. Fagan RP, Fairweather NF. 2011. *Clostridium difficile* has two parallel and essential sec
671 secretion systems. J Biol Chem 286:27483–27493.
672

Figure 1

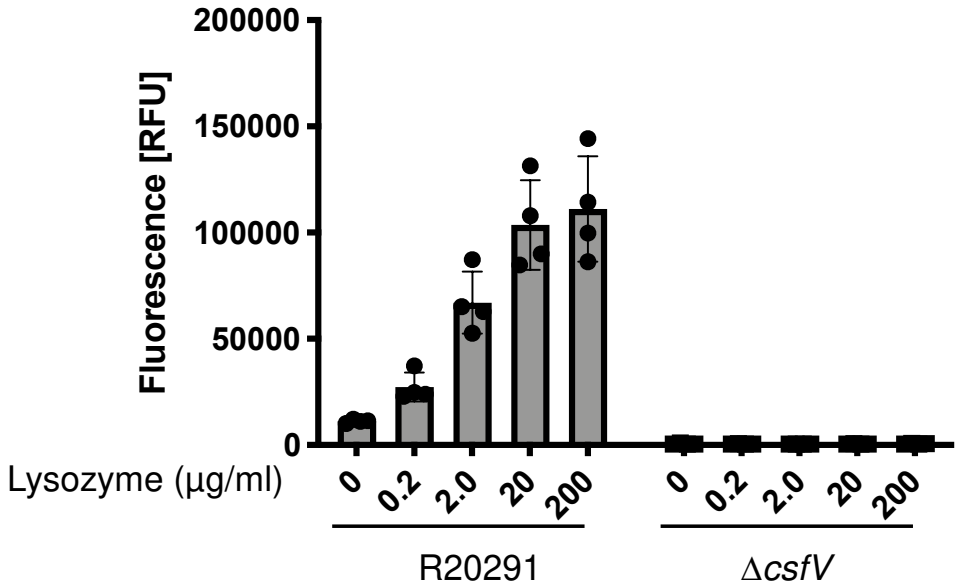

Figure 1. Wildtype (GMK208) or Δ*csfV* (GMK211) strains containing a P_{pdaV}-*rfp* reporter plasmid were grown to an OD_{600} of 0.3, incubated with lysozyme for 1 hr, then fixed and removed from the anaerobic chamber. Samples were exposed to air overnight to allow for maturation of the chromophore. Fluorescence was measured via a plate reader.

Figure 2

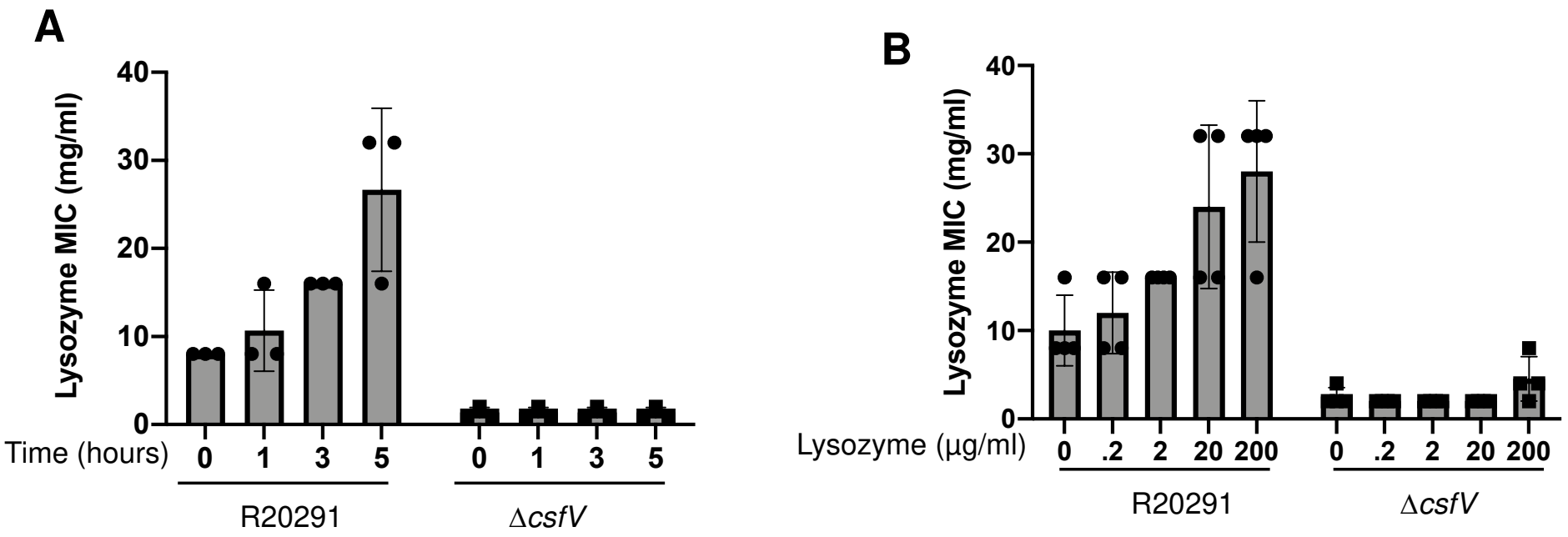

Figure 2. Pre-incubation with a sub-inhibitory concentration of lysozyme increases resistance level. A) Overnight cultures of wildtype or Δ*csfV* (CDE2966) were sub-cultured and grown for ~8hrs; 20 µg/ml lysozyme was added for the duration indicated prior to set up of the lysozyme MIC plates. B) Overnight cultures were sub-cultured and grown to an OD_{600}= 0.3; varying sub-inhibitory concentrations of lysozyme were added as indicated and cultures incubated for ~5 hrs prior to set up of MIC.

Figure 3

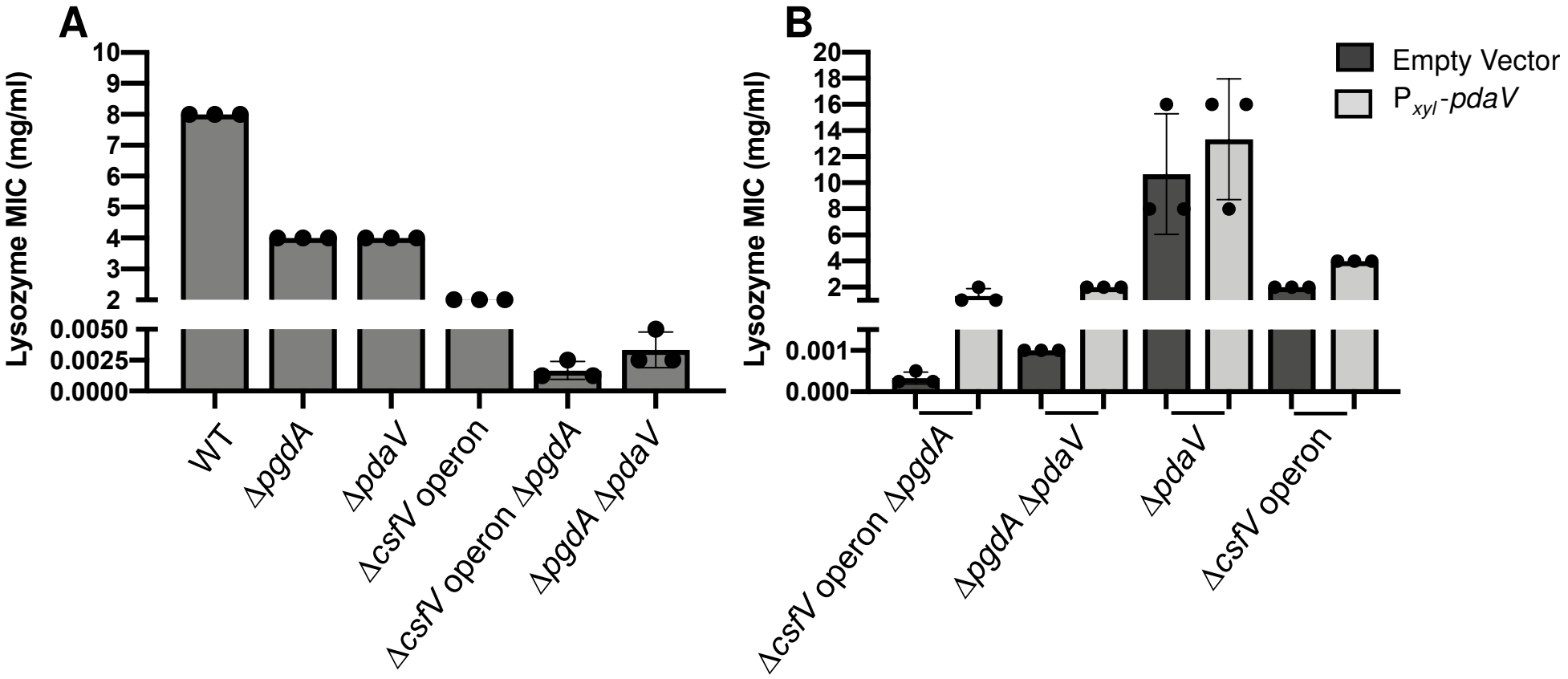

Figure 3. A) Overnight cultures were sub-cultured into TY medium and grown to an OD_{600}= 0.3; 20 μg/ml lysozyme was added and incubated for 5 hrs prior to set up of MIC (WT, R20291; *ΔpgdA,* GMK241; *ΔpdaV,* GMK152; *ΔcsfV* operon, GMK157; *ΔcsfV* operon *ΔpgdA,* GMK243; *ΔpdaV ΔpgdA,* GMK301). B) Strains carrying either P_{xyl}-*pdaV* (pCE618) or an empty vector (pAP114) were constructed (*ΔcsfV* operon *ΔpgdA* pAP114, GMK312; *ΔcsfV* operon *ΔpgdA* pCE618, GMK313; *ΔpdaV ΔpgdA* pAP114, GMK314; *ΔpdaV ΔpgdA* pCE618, GMK315; *ΔpdaV* pAP114, GMK316; *ΔpdaV* pCE618, GMK317; *ΔcsfV* operon pAP114, GMK174; *ΔcsfV* operon pCE618, GMK177). Overnight cultures were sub-cultured into TY Thi_{10} medium supplemented with 1% xylose. Cultures were grown to an OD_{600}= 1.0 and a lysozyme MIC was set up with 1% xylose.

Figure 4

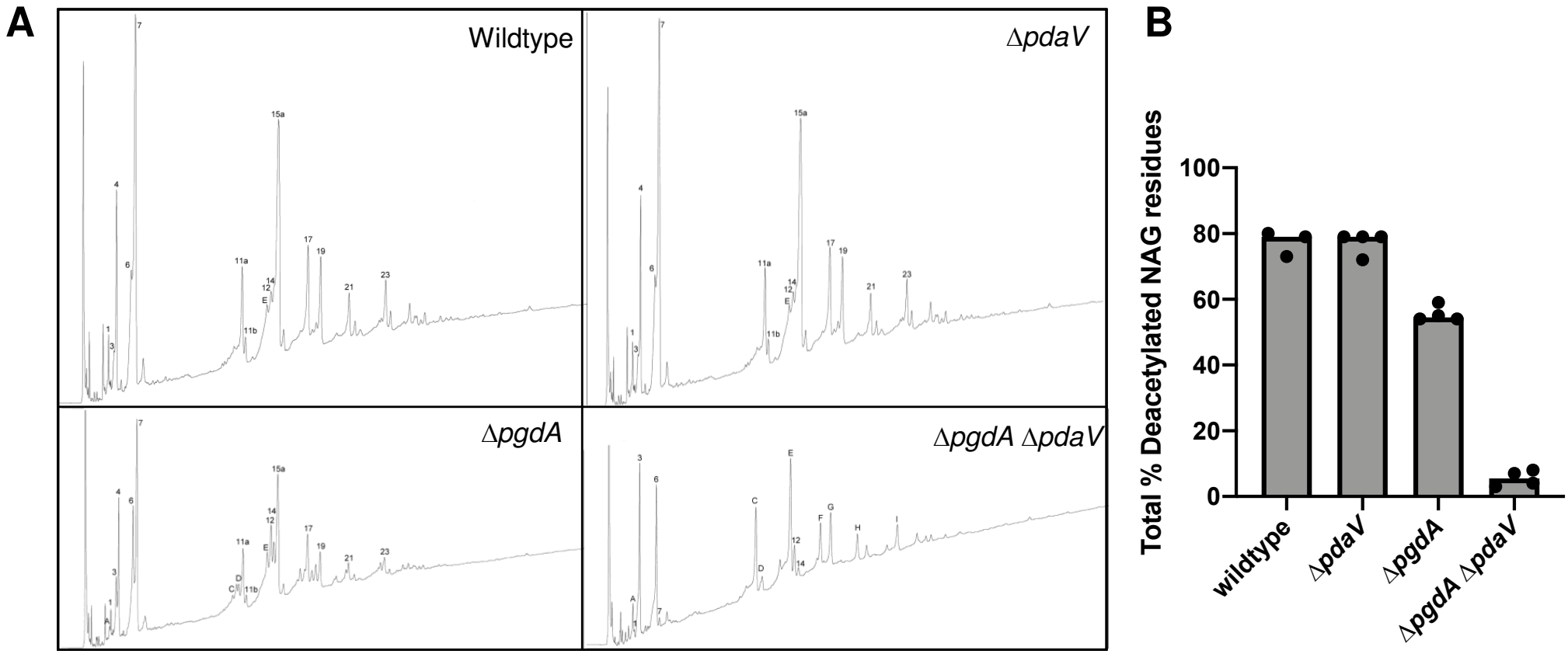

Figure 4. Peptidoglycan was purified from cultures grown to mid-log (OD_{600}= 0.6-0.8). Peptidoglycan was digested with mutanolysin. Fragments were separated using reversed-phase HPLC and structures determined using mass spectrometry. B) Total percentages of deacetylated residues are shown for strains indicated (WT, R20291; *ΔpdaV,* GMK152; *ΔpgdA,* GMK241; *ΔpgdA ΔpdaV,* GMK301).

Figure 5

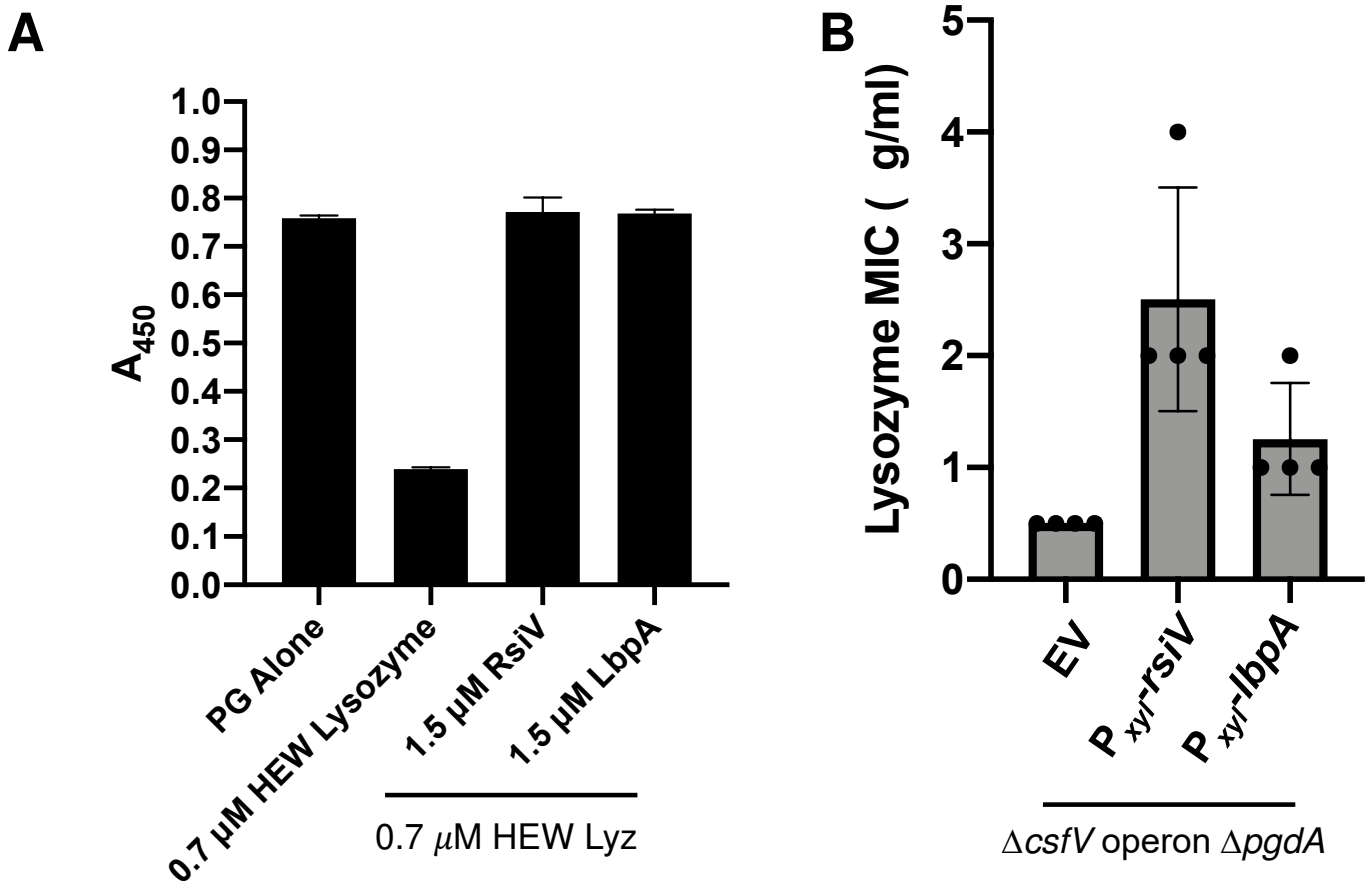

Figure 5. A) Peptidoglycan from *M. lysodeikticus* was combined with 10 µg/ml lysozyme and purified RsiV or LbpA. The A_{450} was monitored every minute for 30 minutes to determine degradation of lysozyme. Degradation after 30 minutes is shown. B) Overnight cultures were sub-cultured into TY Thi_{10} medium supplemented with 1% xylose and grown to OD_{600}= 1.0 and a lysozyme MIC was set up with 1% xylose. A one-way ANOVA showed effect of the inhibitor proteins on lysozyme resistance was significant, F (2,9)= 9.8, *p*= 0.0055.